

421059  
N94-33228

538 91 ABS. ONL

**THE WAVELENGTH DEPENDENCE OF MARTIAN ATMOSPHERIC DUST RADIATIVE PROPERTIES.** J. B. Pollack<sup>1</sup>, M. E. Ockert-Bell<sup>2</sup>, R. Arvidson<sup>3</sup>, and M. Shepard<sup>3</sup>, <sup>1</sup>NASA Ames Research Center, Moffett Field CA 94035-1000, USA, <sup>2</sup>San Jose State University, San Jose CA 95172-0130, USA, <sup>3</sup>Washington University, St. Louis MO 63130-4899, USA.

**Motivation:** One of the key radiative agents in the atmosphere of Mars is the suspended dust particles. We are carrying out a new analysis of two datasets of the martian atmosphere in order to better evaluate the radiative properties of the atmospheric dust particles. The properties of interest are the size distribution information, the optical constants, and other radiative properties, such as the single-scattering albedo and phase function. Of prime importance in this research is the wavelength dependence of these radiative properties throughout the visible and near-infrared wavelengths. Understanding the wavelength dependence of absorption and scattering characteristics will provide a good definition of the influence that the atmospheric dust has on heating of the atmosphere.

**Data:** The first dataset that we are analyzing is a set of Viking 1 and 2 Lander images. Our present work represents a significant improvement over our past analyses [1,2]. Color and IR images and a survey image have been calibrated and a correction for vignetting was added. The vignetting correction reconstructed the saturation near the top of the images and allowed us to use data closer to the Sun, which in turn gives a better definition of the diffraction peak and, thus, the size distribution of the particles. The second dataset is visible and near-infrared data from Bell and Mustard [3] and Mustard and Bell [4]. The dataset, taken in 1988 and 1989, covers a wide range of wavelengths (0.4–3.0  $\mu\text{m}$ ).

**Analysis:** The examination of the Viking Lander images involves modeling the reflectance data using radiative transfer calculations based on the doubling method [5]. A semi-empirical method is used to model the scattering by nonspherical particles [6]. Hapke [7,8] theory is used to model the photometric properties of the surface.

We used an iterative method to fit the parameters of interest to the observed data: small phase angles were used to find the size distribution information, phase angles of about  $50^\circ$  were used to determine the imaginary index, and the data at larger phase angles determined the shape of the particles. We calculate the intensity expected in a given range due to variation of one parameter and do a chi-squared fit to the variance to find the best fit of the parameter in question. The resulting best fit is used as a set parameter while another is varied, etc.

From the information obtained in the examination of the Viking Lander images, we have defined the particle size distribution using a log-normal distribution, and we have defined the wavelength dependence of the imaginary index of refraction and radiative properties for wavelengths between 0.5 and 0.9  $\mu\text{m}$ .

For the investigation of the second dataset we operate under the assumption that the properties of the atmospheric dust closely mimic those of the "bright" soil on the surface. Since the optical depth of the atmospheric dust was low during the time period of the data acquisition, we can use Hapke theory [7,8] to extract the single-scattering albedo of the soil. By scaling the imaginary index of refraction of the soil to agree with the atmospheric dust in the visible, we derive the spectral dependence of the imaginary index in the entire visible and near-infrared domains.

The results of this inquiry will be presented. The particle single-scattering phase function from the Viking analysis and the wavelength dependence of the radiative properties within the visible and near-infrared wavelength regions will be given.

**References:** [1] Pollack J. B. et al. (1977) *JGR*, 82, 4479–4496. [2] Pollack J. B. et al. (1979) *JGR*, 84, 2929–2945. [3] Bell J. F. III and Mustard J. F. (1993) *LPSXXIV*, 81–82. [4] Mustard J. F. and Bell III J. F. (1993) *GRL*, submitted. [5] Hansen J. E. (1969) *Astrophys. J.*, 155, 565. [6] Pollack J. B. and Cuzzi J. N. (1980) *JAS*, 37, 868–881. [7] Hapke B. (1981) *JGR*, 86, 3039–3054. [8] Hapke B. (1986) *Icarus*, 67, 264–280.

N94-33229

539 91 ABS.  
**EVIDENCE FOR ULTRAMAFIC LAVAS ON SYRTIS MAJOR.** D. P. Reyes and P. R. Christensen, Department of Geology, Arizona State University, Tempe AZ 85287-1404, USA.

Data from the Phobos 2 Imaging Spectrometer for Mars (ISM) compiled by [1] support the existence of komatiitic lavas on the Syrtis Major plateau. Using ISM data, Mustard et al. [1] determined that the composition of the low-albedo materials covering the Syrtis Major plateau originally consisted of augite-bearing basalt containing two cogenetic pyroxenes with no appreciable amount of olivine. Additionally, Syrtis Major ISM visible and near-infrared spectra were matched to the spectra of an Apollo 12 basalt and a Shergotite meteorite to show that the ISM spectra are consistent with a mafic basalt composition [1]. In this work, pyroxene compositions from ISM data determined by [1] compared with the pyroxene compositions of Apollo 12 pigeonite basalt, Shergotite meteorite, and pyroxenitic komatiite show that the Syrtis Major volcanic materials are consistent with pyroxenitic komatiite. Pyroxenitic komatiite is significant for the Earth because it contains a large amount of MgO, implying generation under unique circumstances compared to typical basaltic compositions [e.g., 2].

**Background:** Komatiites are subdivided by weight percent MgO into peridotitic (>20%), pyroxenitic (12–20%), and basaltic (8–12%) varieties [3]. Pyroxenitic and basaltic komatiites may be collectively referred to as mafic komatiites. Mafic komatiites are always found with peridotitic komatiites in the Archean and are also found alone in the few Proterozoic occurrences. Peridotitic komatiites are dominated by olivine, with interstitial clinopyroxene and glass. Mafic komatiites are dominated by pyroxene (augite  $\pm$  pigeonite  $\pm$  bronzite), with lesser plagioclase, and rare olivine. Olivine is only present in a few mafic komatiite flows where MgO content is >12% and even then olivine only accounts for <10% of the mode [4].

The upper portion of pyroxenitic komatiite flows are often composed of skeletal magnesium pigeonite with augite exteriors in a fine augite and plagioclase groundmass. Coexisting magnesium pigeonite and augite are unusual for most lavas on the Earth, but are an important characteristic of pyroxenitic komatiites [4]. According to Campbell and Arndt [5], rapid cooling in the upper parts of some komatiite flows may cause olivine to crystallize initially. However, the rate of olivine crystallization is not sufficient to prevent continued supercooling of the liquid to a point below the temperature of the stable pyroxene liquidus. This supercooling results in the crystallization of magnesian pigeonite in a liquid that would normally produce olivine under equilibrium conditions. As the liquid temperature drops further, augite crystallizes, followed by plagioclase.

Coexisting pigeonite and augite are also found in ~12 categories of lunar mare basalts and well-developed skeletal pigeonite mantled by augite is found in Apollo 15 and Apollo 12 pigeonite basalts [6]. All 12 of these basalt groups are magnesium rich, ranging in weight percent MgO from 7.03% to 19.97%, and averaging 10.7% [6]. Like komatiites, the coexisting pyroxenes in the Apollo 12 pigeonite basalts are thought to form by rapid metastable crystallization of a supercooled liquid [7]. Regardless of the specific mechanism that forms skeletal textures and coexisting pigeonite and augite, these features are characteristic of highly magnesian lavas like komatiites.

**Discussion:** Using ISM data, Mustard et al. [1] estimated the composition of Syrtis Major pyroxenes. According to Mustard et al., the pyroxene compositions represented by their ISM analysis falls in an area of "unusual" composition on the pyroxene quadrilateral, and therefore the data may represent an average composition of augite and pigeonite as intimate exsolution lamella. Telescopic reflectance measurements of several dark regions on Mars are indicative of coexisting pyroxenes, which correlates with the modal mineralogy of Shergotite meteorites, which may have originated from Mars [8]. Comparison with Shergotite meteorites and terrestrial komatiites suggests that exsolution lamella are not required by the results of [1]. If the ISM data represent an average of two pyroxene compositions, then discrete pyroxenes may be implied. Furthermore, if coexisting pyroxenes were detected by the ISM on Syrtis Major, then they may have formed by a mechanism like that previously described for the crystallization of pyroxenes in mafic komatiite and Apollo 12 pigeonite basalts.

Figure 1 shows a pyroxene quadrilateral with the Syrtis Major ISM pyroxene field of [1] superposed over the compositions of pyroxenes found in a pyroxenitic komatiite flow, the Shergotite meteorite, and an Apollo 12 pigeonite basalt. The majority of pyroxenitic komatiite pyroxene analyses do not fall within the ISM field because their source liquid contained relatively little Fe compared to potential martian lavas [e.g., 3,9]. Many individual pyroxene analyses from the Shergotite and the Apollo 12 pigeonite basalt do fall within the ISM field. More importantly, the averaged composition of coexisting pyroxenes in the plotted samples will also fall within the ISM field. These samples perform better than the komatiite because the higher Fe content in these rocks allows greater substitution of Fe in the pyroxene structure as Mg is consumed initially. A crystallization trend is defined that places these pyroxene analy-

ses within and below the ISM field, as seen in Fig. 1. This analysis supports the possibility of komatiite-type lava on the Syrtis Major plateau because these coexisting pyroxenes are indicative of magnesian komatiite-type lava.

An important caveat to the analysis presented here and to that of [1] is that Syrtis Major plateau is composed of a large sand sheet and dune field, with varying degrees of variable fine-grained dust coatings [1]. The question arises whether the materials observed represent locally derived or transported materials. Additionally, if local or distal in origin, certain phases in the Syrtis Major material may have been preferentially concentrated by eolian activity or chemical weathering. The relatively low spatial resolution of ISM (24 km) makes these questions difficult to answer.

A thermal emission spectrometer (TES) with a spectral resolution of 5–10 cm<sup>-1</sup>, from 5 to 60 μm, and a spatial resolution of 3 km (e.g. the Mars Observer Thermal Emission Spectrometer [10]), would easily reveal the presence and nature of komatiitic lavas on Syrtis Major as indicated by the evidence discussed. In addition, TES-type data could be used to study weathering products and to trace sediment transport paths in an attempt to distinguish primary igneous materials from reworked sediments. Finally, a TES would reveal if Syrtis Major lava composition evolves from peridotitic to basaltic compositions over time as seen in terrestrial komatiites [3].

**References:** [1] Mustard J. F. et al., (1993) *JGR*, 98, 3387–3400. [2] Takahashi E. (1991) *JGR*, 95, 15941–15954. [3] Arndt N. T. et al. (1977) *J. Pet.*, 18, 319–369. [4] Cameron W. E. and Nisbet E. G. (1982) In *Komatiites* (Arndt N. T. and Nisbet E. G., eds.), George Allen and Unwin, Boston, 29–50. [5] Campbell I. H. and Arndt N. T. (1982) *Geol. Mag.*, 119, 605–610. [6] *BVSP, Basaltic Volcanism Study Project* (1981) Pergamon, New York, 1286 pp. [7] Klein C. et al. (1971) *Proc. LSC 2nd*, 265–284. [8] Straub D. W. et al. (1991) *JGR*, 96, 18819–18830. [9] McGetchin T. R. and Smyth J. R. (1978) *Icarus*, 34, 512–536. [10] Christensen P. R. et al. (1992) *JGR*, 97, 7719–7734

N94-33230

54091 ABS ONLY  
**MARTIAN DELTAS: MORPHOLOGY AND DISTRIBUTION.** J. W. Rice Jr.<sup>1</sup> and D. H. Scott<sup>2</sup>, <sup>1</sup>Department of Geography, Arizona State University, Tempe AZ 85283, USA, <sup>2</sup>Astrogeology Branch, U.S. Geological Survey, 2255 N. Gemini Drive, Flagstaff AZ 86001, USA.

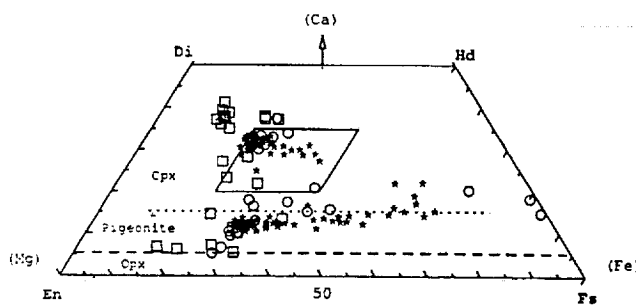


**Fig. 1.** Pyroxene compositions from Syrtis Major ISM and analogs. ISM field (rhomboid) from [1]; pyroxenitic komatiite data (squares) provided by D. P. Reyes, [sample DPY-10, unpublished data, Reyes, 1993]; and Apollo 12 pigeonite basalt (circles) and Shergotite meteorite (stars) data from [6].

The identification of deltas on Mars has been an enigma over the years for planetary geologists. However, recent detailed mapping (1:500,000 scale) has revealed numerous examples of martian deltas. We will document and describe the location and morphology of these deltas.

Deltas are alluvial regions composed of sediment deposited in relatively still water (lakes, bays, seas) at river mouths. Deposition on deltas occurs when river velocity is reduced upon entering standing bodies of water. Factors that contribute to delta morphology are river regime, coastal processes, structural stability, and climate [1].

The largest delta systems on Mars are located near the mouths of Maja, Maumee, Vedra, Ma'adim, Kasei, and Brazos Valles. There are also several smaller-scale deltas emplaced near channel mouths situated in Ismenius Lacus, Memnonia, and Arabia.

Delta morphology will be used to reconstruct type, quantity, and sediment load size transported by the debouching channel systems